JOURNAL OF SOLID STATE CHEMISTRY 120, 260–267 (1995)

A Molybdenum V Diphosphate Involving LiO_4 Tetrahedra: $LiMoOP_2O_7$

S. Ledain, M. M. Borel, A. Leclaire, J. Provost, and B. Raveau

Laboratoire CRISMAT, URA 1318 associé au CNRS, ISMRA et Université de Caen, Boulevard du Maréchal Juin, 14050 Caen Cedex, France

Received February 22, 1995; accepted July 19, 1995

A lithium Mo(V) diphosphate $LiMoOP_2O_7$ has been synthesized for the first time. It crystallizes in the space group $P2_{1/n}$ with $a = 16.046$ (4) Å, $b = 11.951$ (2) Å, $c = 9.937$ (2) Å, $\beta = 104.62$ (2)°. Its original structure is built up from P_2O_7 groups and MoO_6 octahedra forming intersecting tunnels, where the Li^+ cations are located with a tetrahedral coordination. This phase belongs to the IB class of Mo(V) phosphates defined by Costentin *et al.* The $[MoP_2O_8]$ framework indeed consists of MoP_2O_{11} units built up from one P_2O_7 group sharing two apices with the same MoO_6 octahedron; the MoP_2O_{11} units share their apices forming $[MoP_2O_{10}]_\infty$ chains running along a and b and the $[\bar{1}04]$ direction. This phase exhibits a classical paramagnetic behavior, with $\theta = -9.8$ K and $\mu = 1.58\ \mu_B$.

INTRODUCTION

The studies of molybdenophosphates performed in the past 10 years have shown the existence of a large series of Mo(V) phosphates, with different and original host lattices, in which various cations such as sodium, potassium, rubidium, thallium, cesium, and barium are interpolated (see for a review Ref. (1–2)). Most of these structures are characterized by the presence of tunnels, which originate from the particular behavior of Mo(V). The electronic configuration of the latter favors the formation of an abnormally short molybdenyl Mo–O bond, so that each Mo^VO_6 octahedron exhibits a free apex. This results in extraordinary flexibility of the molybdenum–oxygen framework which can accommodate a large variety of cations. Curiously, no Mo(V) lithium phosphate has been synthesized up to date, to our knowledge. Nevertheless, there exists a mixed valent molybdenum phosphate, $LiMo_2^VMo^{VI}P_3O_{16}$ (3), isotypic to the sodium and silver phases (4, 5). For this reason we have investigated the system Li–Mo(V)–P–O. We report here on the crystal structure and magnetic characteristics of the first Mo(V) lithium phosphate $LiMo^VOP_2O_7$.

EXPERIMENTAL

Single crystals of the title compound were grown from a mixture of nominal composition $Li_3Mo_4P_5O_{20}$. This compound has been synthesized in two steps: first $H(NH_4)_2PO_4$, Li_2CO_3, and MoO_3 were mixed in agate mortar in adequate ratios according to the composition $Li_3Mo_2P_5O_{20}$ and heated at 600 K in a platinum crucible to decompose the ammonium phosphate and lithium carbonate. In a second step, the resulting mixture was added to the required amount of molybdenum (2 mole) placed in an alumina tube and sealed in an evacuated silica ampoule, then heated for 24 hr at 973 K, and cooled at 9 K per hr to 298 K. Blue crystals corresponding to $LiMoOP_2O_7$ were extracted from the resulting product. Their composition was also confirmed by microprobe analysis. Subsequently, a reaction to prepare pure powder $LiMoOP_2O_7$ was carried out at 873 K for 24 hr and quenched to room temperature. The powder X-ray diffraction pattern (Table 1) of this phosphate was indexed in a monoclinic cell (Table 2) in agreement with the parameters obtained from the single crystal X-ray study.

STRUCTURE DETERMINATION

A blue crystal with dimensions $0.06 \times 0.05 \times 0.03$ mm^3 was selected for the structure determination. The cell parameters reported in Table 2 were determined and refined by diffractometric techniques at 294 K with a least squares refinement based upon 25 reflections with $18° \leq \theta \leq 22°$. The data were collected on a CAD4 Enraf Nonius diffractometer with the data collection parameters of Table 2. The systematic extinctions $h + l = 2n + 1$ for $h\ 0\ l$ and $k = 2n + 1$ for $0\ k\ 0$ are characteristic of the space group $P2_{1/n}$. The diffraction reflections with $h \neq 3n$ are very weak showing a pseudo-translation of $a/3$ in the structure.

The reflections were corrected for Lorentz and polarization effects.

Atomic coordinates of the molybdenum atoms were deduced from the Patterson function and the other atoms were located by subsequent Fourier series.

0022-4596/95 $12.00

TABLE 1
X-Ray Powder Diffraction Data of $LiMoOP_2O_7$

h	k	l	d_{obs} (Å)	d_{calc} (Å)	I
2	0	0	7.766	7.763	5
1	0	1	7.391	7.383	6
0	2	0	5.975	5.975	62
3	0	−1	5.129	5.129	33
0	0	2	4.805	4.807	43
3	1	0	4.750	4.749	32
0	1	2	4.450	4.460	9
2	1	−2	4.322	4.330	3
3	0	1	4.137	4.141	61
2	2	1	4.014	4.013	4
3	1	1	3.913	3.913	100
3	1	−2	3.855	3.854	12
0	2	−2	3.749	3.745	5
0	3	−1	3.678	3.680	46
2	1	2	3.522	3.527	6
3	2	1	3.402	3.404	57
3	2	−2	3.367	3.365	10
4	2	0	3.256	3.255	45
2	3	1	3.208	3.207	5
3	3	−1	3.147	3.146	26
0	1	−3	3.096	3.095	13
5	1	0	3.002	3.005	70
1	4	0	2.943	2.933	20
0	4	−1	2.853	2.853	37
5	2	−1	2.820	2.821	5
2	3	2	2.706	2.707	5
6	0	0	2.588	2.588	11
3	4	0	2.588	2.587	11
6	0	−2	2.565	2.564	4
0	4	2	2.534	2.537	8
0	3	3	2.499	2.497	9
3	3	2	2.471	2.470	9
3	3	−3	2.443	2.445	4
6	2	−1	2.443	2.440	4
3	1	3	2.410	2.410	18
6	2	0	2.375	2.374	9
6	2	−2	2.357	2.357	22
2	4	2	2.321	2.322	3
6	1	−3	2.278	2.277	2
4	4	1	2.225	2.221	21
2	5	1	2.186	2.186	7
3	4	2	2.167	2.167	5
3	3	3	2.093	2.093	5
6	2	1	2.040	2.040	44
4	5	0	2.035	2.035	26
6	2	2	1.956	1.957	10
6	4	0	1.956	1.956	10
8	1	0	1.915	1.916	12
5	5	−1	1.915	1.915	12
1	4	−4	1.904	1.904	10
3	6	0	1.859	1.858	10
6	3	2	1.837	1.837	10

Refinement of the atomic coordinates and their anisotropic thermal parameters for molybdenum and isotropic factors for the other atoms led to $R = 0.034$ $R_w = 0.037$, and the atomic parameters of Table 3.

TABLE 2
Summary of Crystal Data, Intensity Measurements, and Structure Refinement Parameters for $LiMoOP_2O_7$

Crystal data	
Space group	$P2_{1/n}$
Cell dimensions	$a = 16.046(4)$Å $b = 11.951(2)$ Å $\beta = 104.62(2)°$ $c = 9.937(2)$Å
Volume (Å)^3	1844.8(6)
Z	12
ρ_{calc} (g cm^3)	3.16
Intensity measurements	
λ(Mo$K\alpha$)	0.71073
Scan mode	$\omega - \theta$
Scan width(°)	1. + 0.35 tn θ
Slit aperture (mm)	0.9 + tn θ
Max θ(°)	37
Standard reflections	3 measured every 3600 sec
Measured reflections	10121
Reflections with $I > 3\sigma$	1415
μ(mm^{-1})	2.60
Structure solution and refinement	
Parameters refined	159
Agreement factors	$R = 0.034$ $R_w = 0.037$
Weighting scheme	$w = f(\sin\theta/\lambda)$
Δ/σ max	<0.02
$\Delta\rho$	<0.9

DESCRIPTION OF THE STRUCTURE AND DISCUSSION

The projection of the structure of this new diphosphate along [100] (Fig. 1) shows that the $[MoP_2O_8]_\infty$ framework consists of corner-sharing MoO_6 octahedra and P_2O_7 groups forming octahedral an bitetrahedral files along **a**. These files linked together delimit two sorts of tunnels running along **a**: six-sided tunnels which are empty and ten-sided tunnels where the Li^+ cations are located.

The framework can easily be described from the stacking along **b** of identical $[MoP_2O_9]_\infty$ layers parallel to [010] (Fig. 2). Each layer is built from MoP_2O_{11} units in which one P_2O_7 group shares two of its corners with the same MoO_6 octahedron. Such a unit has already been observed in the Mo(III) diphosphates $AMoP_2O_7$ (A = Na, K, Rb, Tl, Cs) (6–10) and in the Mo(V) phosphates $AMo_2P_3O_{13}$ (A = Na, Ag, K, Rb, Tl, Cs) (11–18) and $Ba(MoO)_2(P_2O_7)_2$ (19). In $LiMoOP_2O_7$, the MoP_2O_{11} units share the corners of their polyhedra, so that they form $[MoP_2O_{10}]_\infty$ chains running along the [$\bar{1}$04] direction. In these chains, each tetrahedron of one unit is linked to one octahedron of the next MoP_2O_{11} unit, forming $[MoPO_8]_\infty$ chains in which one octahedron alternates with one tetrahedron (Fig. 2). One tetrahedron of one $[MoPO_8]_\infty$ chain shares one apex with one octahedron of the adjacent chain and vice versa forming the $[MoP_2O_9]_\infty$ layer. The $[MoP_2O_{10}]_\infty$ chains delimit S-shaped windows built up from five MoO_6 octahedra and

TABLE 3
Positional Parameters and Their Estimated Standard Deviations

Atom	x	y	z	B (Å2)
Mo(1)	0.23712(7)	0.19528(9)	0.1878(1)	0.43(1)[a]
Mo(2)	0.57656(8)	0.21664(8)	0.1992(1)	0.41(2)[a]
Mo(3)	0.90907(7)	0.2023(1)	0.1932(1)	0.44(1)[a]
P(1)	0.1195(2)	0.2968(3)	0.3854(3)	0.42(4)
P(2)	0.1595(2)	0.4500(3)	0.1895(4)	0.34(5)
P(3)	0.4787(2)	0.4582(3)	0.1817(4)	0.49(5)
P(4)	0.4419(2)	0.3008(3)	0.3816(4)	0.68(5)
P(5)	0.3387(2)	0.0415(3)	0.7148(4)	0.61(5)
P(6)	0.3767(2)	0.1741(3)	0.9715(4)	0.48(5)
Li(1)	0.022(2)	0.436(2)	0.902(3)	1.3(2)
Li(2)	0.212(2)	0.064(2)	0.439(3)	1.3
Li(3)	0.355(2)	0.443(2)	0.903(3)	1.3
O(1)	0.1542(7)	0.135(1)	0.079(1)	1.7(2)
O(2)	0.3140(7)	0.191(1)	0.061(1)	1.7(2)
O(3)	0.2846(6)	0.0538(9)	0.295(1)	0.9(2)
O(4)	0.1870(6)	0.2146(8)	0.355(1)	0.7(1)
O(5)	0.2051(7)	0.3546(9)	0.135(1)	1.1(2)
O(6)	0.3494(6)	0.2736(9)	0.324(1)	1.0(2)
O(7)	0.6643(8)	0.272(1)	0.302(1)	2.0(2)
O(8)	0.6309(5)	0.1934(8)	0.0412(9)	0.4(1)
O(9)	0.5002(5)	0.2141(8)	0.333(1)	0.5(1)
O(10)	0.5954(7)	0.051(1)	0.268(1)	1.1(2)
O(11)	0.5200(6)	0.3601(8)	0.124(1)	0.7(2)
O(12)	0.4652(6)	0.1427(9)	0.054(1)	0.9(2)
O(13)	0.8159(7)	0.1470(9)	0.110(1)	1.2(2)
O(14)	0.9692(6)	0.1905(9)	0.038(1)	0.7(1)
O(15)	0.9523(6)	0.0529(8)	0.283(1)	0.7(2)
O(16)	0.8735(6)	0.2235(8)	0.377(1)	0.6(1)
O(17)	0.8793(6)	0.3633(9)	0.149(1)	0.8(2)
O(18)	1.0307(6)	0.2707(9)	0.301(1)	1.0(2)
O(19)	0.1486(6)	0.4164(8)	0.340(1)	0.3(1)
O(20)	0.0707(6)	0.4723(8)	0.097(1)	0.7(1)
O(21)	0.4651(6)	0.4197(9)	0.329(1)	0.9(2)
O(22)	0.3981(8)	0.490(1)	0.085(1)	2.0(2)
O(23)	0.3373(7)	0.0736(9)	0.870(1)	1.0(2)
O(24)	0.2504(7)	0.0120(9)	0.634(1)	1.2(2)

[a] Atoms were refined anisotropically. Anisotropically refined atoms are given in the form of the isotropic equivalent displacement parameter defined as $B = 4/3 \sum_i \sum_j \mathbf{a}_i\mathbf{a}_j\beta_{ij}$.

five PO_4 tetrahedra. Note that the tetrahedra that form the $[MoPO_8]_\infty$ chains (P(1),P(4)P(6)) share three apices with the MoO_6 octahedra and one apex with one PO_4 tetrahedron (P(2)P(3)P(5)). The second kind of PO_4 tetrahedron (P(2),(P3)(P5)) shares one apex with one PO_4 tetrahedron, one MoO_6 octahedron within the $[MoP_2O_{10}]_\infty$ chain, and a third apex with an octahedron of a $[MoP_2O_{10}]_\infty$ chain located either above or below its own chain, its fourth apex being free. Thus, the connection between the $[MoP_2O_9]_\infty$ layers is ensured through this second kind of tetrahedra, leading to the tridimensional framework $[MoP_2O_8]_\infty$, whose projection along **b** (Fig. 3) shows S-shaped tunnels running along **b**, with the free apices of the MoO_6 octahedra and PO_4 tetrahedra directed toward the center of the tunnels.

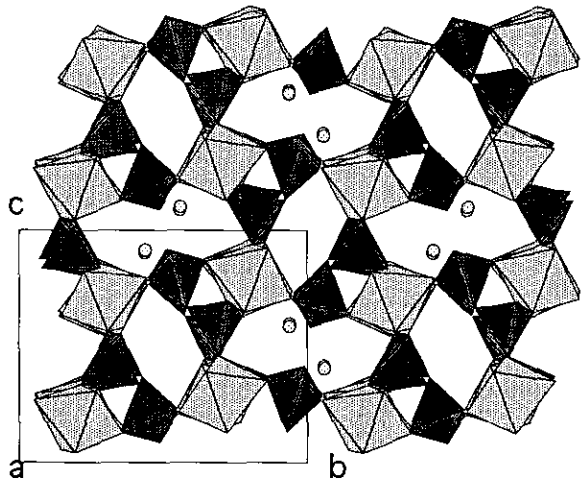

FIG. 1. Projection along **a** of the structure of $LiMoP_2O_8$ showing two sorts of tunnels.

The projections of this structure along **a** (Fig. 1) and along **c** (Fig. 4) show that $[MoP_2O_{10}]_\infty$ chains built up from corner-sharing MoP_2O_{11} units (Fig. 5) are also running along **b** and **a**. The projection along **c** shows also two sorts of tunnels running along that direction, that are occupied by lithium. Thus it appears that the $[MoP_2O_8]_\infty$ framework forms intersecting tunnels running along the three crystallographic directions **a**, **b**, and **c**. Note however, that the

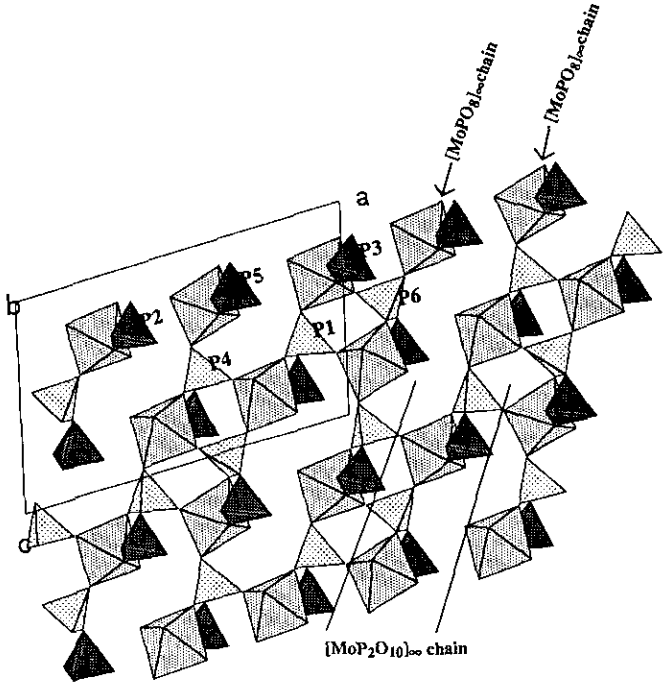

FIG. 2. The $[MoP_2O_9]$ layer showing the $[MoP_2O_{10}]$ chains running along [104] built up from $[MoPO_8]$ chains (identified by the light hatched tetrahedra) sharing two corners with the other tetrahedra.

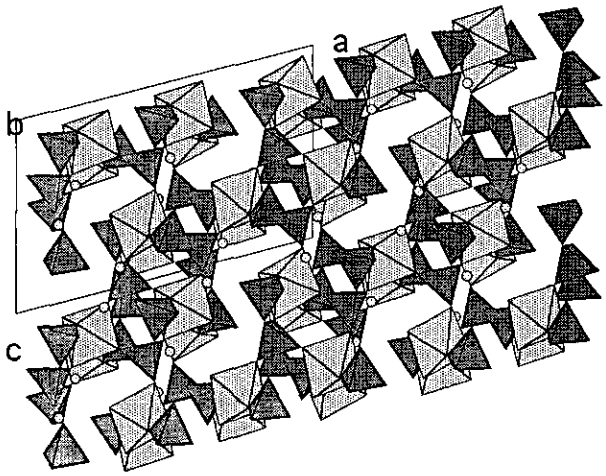

FIG. 3. The projection along **b** showing the S-shaped windows and the P(6) O_4 tetrahedra which destroys the *a*/3 translation induced by the other polyhedra.

size of these tunnels is relatively small, compared to other alkaline phosphates.

The projections of the structure along **b** (Figs. 2 and 3) and **c** (Fig. 4) clearly show that there exists a crystallographic subcell with $a' = a/3$, which corresponds to the translations of the majority of the atoms. The tripling of the a' parameter is due to the fact that one PO_4 group (P6) out of six does not obey the **a**/3 translation.

Thus, the structure of $LiMoOP_2O_7$ observed is very different from the two other Mo(V) diphosphates $KMoOP_2O_7$ (20) and $CsMoOP_2O_7$ (21) that also exhibit P_2O_7 groups with a free apex, but for which the MoP_2O_{11} units are not observed. In contrast, $LiMoOP_2O_7$ belongs to the IB class of Mo(V) phosphates defined by Costentin *et al.* (2), in which the MoP_2O_{11} units share their corners to form infinite $[MoP_2O_{10}]_\infty$ chains similar to those described here for $LiMoOP_2O_7$ (Fig. 5). Such chains are indeed observed

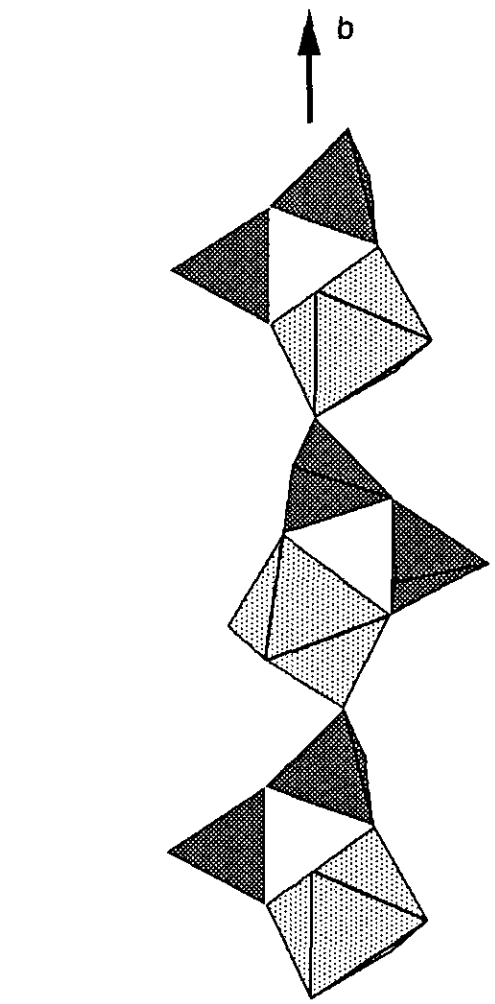

FIG. 5. The $[MoP_2O_{10}]$ infinite chains running along **b**.

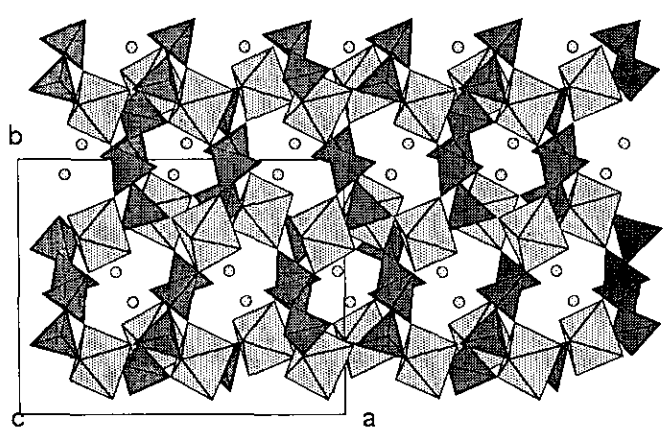

FIG. 4. Projection along **c** of $LiMoP_2O_8$ showing tunnels filled by Li atoms.

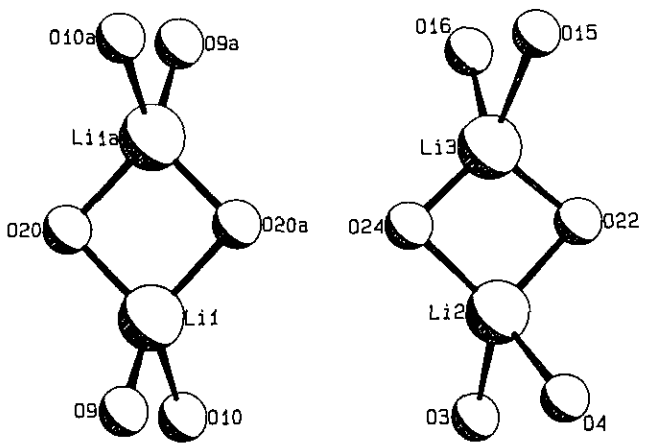

FIG. 6. The tetrahedral oxygen surrounding the Li cations forming Li_2O_6 bitetrahedral units.

TABLE 4
Distances (Å) and Angles (°) in the Polyhedra

Mo(1)	O(1)	O(2)	O(3)	O(4)	O(5)	O(6)
O(1)	1.65(1)	2.70(2)	2.77(2)	2.83(2)	2.76(2)	3.82(2)
O(2)	95.8(7)	1.98(2)	2.98(2)	3.98(2)	2.84(2)	2.72(2)
O(3)	96.5(6)	95.9(6)	2.04(1)	2.64(2)	4.01(2)	2.81(2)
O(4)	99.5(7)	164.6(6)	80.7(6)	2.04(2)	2.83(2)	2.79(2)
O(5)	97.6(6)	90.9(7)	163.8(6)	88.8(6)	2.01(1)	2.76(2)
O(6)	177.6(7)	81.8(6)	83.6(5)	82.9(5)	82.65(6)	2.17(1)
Mo(2)	O(7)	O(8)	O(9)	O(10)	O(11)	O(12)
O(7)	1.65(2)	2.68(2)	2.82(2)	2.84(2)	2.75(2)	3.83(2)
O(8)	93.8(7)	2.00(2)	4.00(2)	3.00(2)	2.92(2)	2.76(2)
O(9)	99.4(7)	166.2(5)	2.03(1)	2.65(2)	2.80(2)	2.82(2)
O(10)	98.3(6)	94.1(6)	80.3(5)	2.09(1)	4.03(2)	2.80(2)
O(11)	97.2(6)	94.1(6)	88.1(5)	161.9(5)	2.00(1)	2.77(2)
O(12)	176.4(6)	82.6(5)	84.2(5)	82.0(5)	83.1(5)	2.18(1)
Mo(3)	O(13)	O(14)	O(15)	O(16)	O(17)	O(18)
O(13)	1.65(1)	2.78(2)	2.67(2)	2.74(2)	2.77(2)	3.80(2)
O(14)	97.7(6)	2.02(2)	3.01(2)	4.06(2)	2.90(2)	2.73(2)
O(15)	91.9(6)	95.5(6)	2.04(5)	2.69(2)	4.02(2)	2.88(2)
O(16)	94.4(6)	167.9(5)	82.1(5)	2.06(1)	2.83(2)	2.86(2)
O(17)	98.0(6)	91.8(6)	166.8(6)	88.5(5)	2.00(1)	2.75(2)
O(18)	178.9(5)	81.9(6)	87.1(5)	86.1(5)	83.1(5)	2.14(1)
P(1)	O(4)	O(8)^{i}	O(18)^{ii}	O(19)		
O(4)	1.55(1)	2.50(2)	2.52(2)	2.48(2)		
O(8)^{i}	109.7(8)	1.52(2)	2.56(2)	2.47(2)		
O(18)^{ii}	112.0(7)	116.2(8)	1.49(1)	2.53(2)		
O(19)	104.1(7)	104.7(7)	109.4(7)	1.60(1)		
P(2)	O(3)^{iii}	O(5)	O(19)	O(20)		
O(3)^{iii}	1.52(1)	2.47(2)	2.52(2)	2.50(2)		
O(5)	108.8(9)	1.53(2)	2.54(2)	2.52(2)		
O(19)	108.3(8)	108.7(8)	1.60(2)	2.51(2)		
O(20)	111.1(8)	112.1(8)	107.8(8)	1.51(1)		
P(3)	O(11)	O(15)^{iv}	O(21)	O(22)		
O(11)	1.53(1)	2.48(2)	2.52(2)	2.45(2)		
O(15)^{iv}	106.9(7)	1.56(1)	2.50(2)	2.54(2)		
O(21)	107.2(7)	104.6(8)	1.60(2)	2.54(2)		
O(22)	110.6(9)	114.9(8)	112.1(9)	1.45(2)		
P(4)	O(6)	O(9)	O(14)^{i}	O(21)		
O(6)	1.49(1)	2.50(2)	2.51(2)	2.54(2)		
O(9)	111.0(8)	1.55(1)	2.49(2)	2.49(2)		
O(14)^{i}	114.4(9)	108.9(7)	1.50(2)	2.52(2)		
O(21)	111.3(8)	106.7(7)	104.2(8)	1.59(1)		
P(5)	O(10)^{v}	O(17)^{i}	O(23)	O(24)		
O(10)^{v}	1.51(1)	2.39(2)	2.45(2)	2.53(2)		
O(17)^{i}	103.3(8)	1.54(1)	2.57(2)	2.52(2)		
O(23)	104.5(8)	110.2(7)	1.59(1)	2.51(2)		
O(24)	115.6(8)	113.2(7)	109.5(7)	1.48(1)		
P(6)	O(2)^{vi}	O(12)^{iv}	O(16)^{i}	O(23)		
O(2)^{vi}	1.52(2)	2.51(2)	2.49(2)	2.47(2)		
O(12)^{vi}	113.1(8)	1.50(1)	2.55(2)	2.52(2)		
O(16)^{i}	109.2(8)	114.5(7)	1.54(1)	2.49(2)		
O(23)	105.0(7)	109.1(7)	105.3(6)	1.60(1)		

TABLE 4—*Continued*

Li(1)–O(9)^{i}	1.92(4) Å		
Li(1)–O(10)^{i}	1.99(5) Å		
Li(1)–O(20)^{vii}	1.94(4) Å		
Li(1)–O(20)^{vi}	1.85(4) Å		
Li(2)–O(3)	2.06(4) Å		
Li(2)–O(4)	1.98(3) Å		
Li(2)–O(22)^{viii}	1.94(3) Å		
Li(2)–O(24)	1.98(4) Å		
Li(3)–O(15)^{i}	2.19(5) Å		
Li(3)–O(16)^{i}	2.04(4) Å		
Li(3)–O(22)^{vi}	1.86(5) Å		
Li(3)–O(24)^{ix}	1.84(4) Å		
P(1)–O(19)–P(2)	126.7(8)°	P(1)–P(2)	2.860(7) Å
P(3)–O(21)–P(4)	130.8(9)°	P(3)–P(4)	2.902(7) Å
P(5)–O(23)–P(6)	134.0(9)°	P(5)–P(6)	2.933(6) Å

Symmetry code

^{i} $x - \frac{1}{2}; \frac{1}{2} - y; \frac{1}{2} + z$
^{ii} $x - 1; y; z$
^{iii} $\frac{1}{2} - x; \frac{1}{2} + y; \frac{1}{2} - z$
^{iv} $\frac{3}{2} - x; \frac{1}{2} + y; \frac{1}{2} - z$
^{v} $1 - x; -y; 1 - z$
^{vi} $x; y; 1 + z$
^{vii} $-x; 1 - y; 1 - z$
^{vii} $\frac{1}{2} - x; \frac{1}{2} + y; \frac{1}{2} - z$
^{ix} $\frac{1}{2} - x; \frac{1}{2} + y; \frac{3}{2} - z$

Note. The Mo–O or P–O distances are on the diagonal, above it are the O ⋯ O distances and below are the *O–Mo–O* or *O–P–O* angles.

for $Ba(MoO)_2(P_2O_7)_2$ (19), β-$A(MoO)_2P_2O_7(PO_4)$ (14–17), γ-$Cs(MoO)_2(P_2O_7)(PO_4)$ (18), ε-$Na(MoO)_2P_2O_7(PO_4)$ (11), and ξ-$A(MoO)_2P_2O_7(PO_4)$ (12–13). The most striking similarity deals with $Ba(MoO)_2(P_2O_7)$ (19) which is, like $LiMoOP_2O_7$, built up of $[MoP_2O_{10}]_\infty$ chains only. In both structures the $[MoP_2O_{10}]_\infty$ chains share the apices of their polyhedra in such a way that one tetrahedron of one chain is linked to one octahedron of the other chain, leading to the same formulation for the tridimensional framework $[MoP_2O_8]_\infty$. In the same way, each P_2O_7

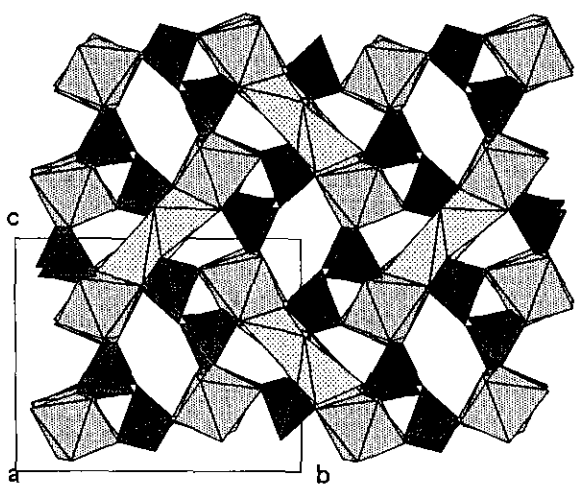

FIG. 7. Projection of the framework along a including the LiO_4 tetrahedra.

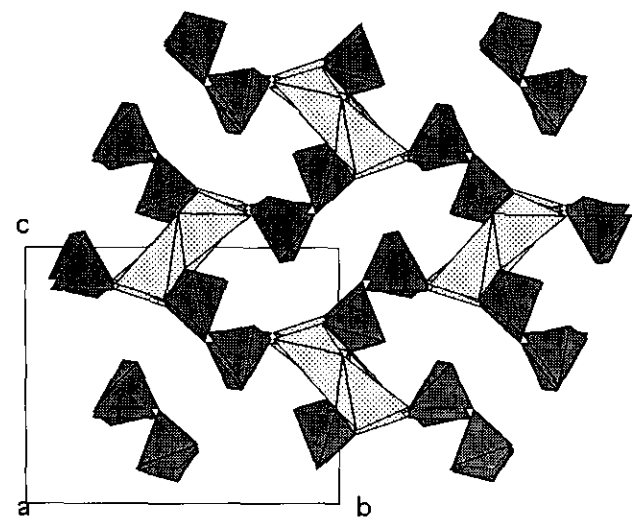

FIG. 8. The LiP_2O_7 tetrahedral three-dimensional framework.

group and each MoO_6 octahedron exhibit one free apex in both structures. Nevertheless the chains are arranged differently in the two compounds.

The three independent molybdenum octahedra exhibit a geometry characteristic of Mo(V); they all have one free apex characterized by a very short Mo–O bond (1.65 Å), the opposite distances are long (2.14–2.18 Å), whereas the intermediate Mo–O bonds are rather homogeneous (1.98–2.09 Å) (Table 4). The sum of the electrostatic valence calculated with a modified Brese and O'Keefe expression for Mo(V) (22) leads to the values 5.08, 4.98, and 5.00 for Mo(1), Mo(2), and Mo(3), respectively. The characteristics of the P_2O_7 groups are very similar to those of the Mo(V) diphosphates $KMoOP_2O_7$ (20), $CsMoOP_2O_7$ (21), and Ba $(MoO)_2(P_2O_7)_2$ (19).

The three Li cations are bonded to four oxygen atoms with Li–O distances ranging from 1.84 to 2.19 Å forming distorded LiO_4 tetrahedra. In the tunnel running along **a**, two LiO_4 tetrahedra share one edge with forming bitetrahedral units (Fig. 6).

Each Li_2O_6 unit shares two opposite edges with MoO_6 octahedra so that $Mo_2Li_2O_{14}$ units are observed (Fig. 7). But the most interesting feature deals with the fact that the Li_2O_6 units share their apices with the diphosphate groups, forming a tridimensional tetrahedral framework $[LiP_2O_7]_\infty$ (Fig. 8) whose cavities are occupied by molybdenyl groups "MoO."

The magnetic moment of a powdered sample, made of very small crystals extracted from the preparation, was measured from 4.5 to 300 K with a SQUID magnetometer for an applied field $B = 3000$ G. The sample was first zero field cooled and the magnetic field was applied after the temperature stabilization at 4.5 K.

After correction of the sample holder signal and of the core diamagnetism, the molar susceptibility χ_M and the inverse molar susceptibility χ_M^{-1} were plotted versus the temperature T.

The inverse molar susceptibility curve $\chi_M^{-1}(T)$ (Fig. 9) is fitted with the classical Curie–Weiss law $\chi_M = c/(T - \theta)$, leading to an effective magnetic moment of 1.58 μ_B molybdenum in agreement with the only presence of Mo(V) ($\mu = 1.55$) and to $\theta = -9.8$ K.

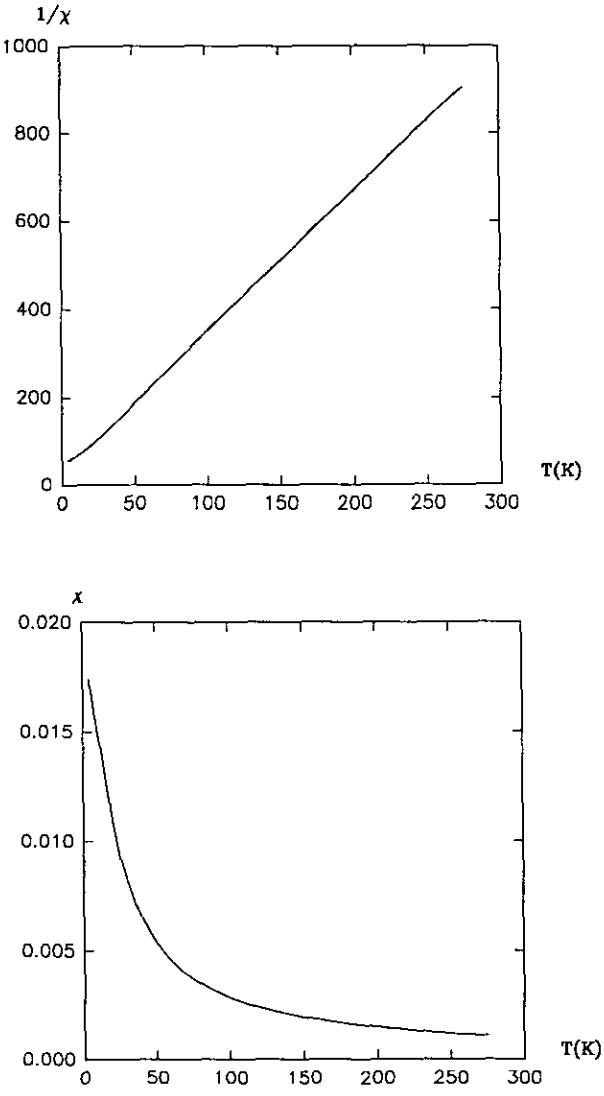

FIG. 9. The magnetic susceptibility χ and $1/\chi$ versus T for $LiMoP_2O_8$.

REFERENCES

1. R. C. Haushalter and L. A. Mundi, *Chem. Mater.* **4,** 31 (1992).
2. G. Costentin, A. Leclaire, M. M. Borel, A. Grandin, and B. Raveau, *Rev. Inorg. Chem.* **13,** 77 (1993).
3. T. Hoareau, M. M. Borel, A. Leclaire, J. Provost, and B. Raveau, *Mat. Res. Bull.,* **30,** 523 (1995).
4. G. Costentin, M. M. Borel, A. Grandin, A. Leclaire, and B. Raveau, *J. Solid State Chem.* **95,** 168 (1991).
5. A. Guesdon, M. M. Borel, A. Grandin, A. Leclaire, and B. Raveau, *C.R. Acad. Sci.* **316,** 477 (1993).
6. A. Leclaire, M. M. Borel, A. Grandin, and B. Raveau, *J. Solid State Chem.* **76,** 131 (1988).
7. A. Leclaire, M. M. Borel, A. Grandin, and B. Raveau, *J. Solid State Chem.* **78,** 220 (1989).
8. J. J. Chen, S. L. Wang, and K. H. Lii, *Acta. Crystallogr. Sect. C* **45,** 673 (1989).
9. D. Riou, A. Leclaire, A. Grandin, and B. Raveau, *Acta. Crystallogr. Sect. C* **45,** 989 (1989).
10. K. H. Lii, and R. C. Haushalter, *Acta. Crystallogr. Sect. C* **43,** 2036 (1987).
11. A. Leclaire, M. M. Borel, A. Grandin, and B. Raveau, *J. Solid State Chem.* **89,** 10 (1990).
12. G. Costentin, M. M. Borel, A. Grandin, A. Leclaire, and B. Raveau, *J. Solid State Chem.* **89,** 31 (1990).
13. T. Hoareau, M. M. Borel, A. Grandin, A. Leclaire, and B. Raveau, *C.R. Acad. Sci.* **319,** 47 (1994).
14. A. Leclaire, M. M. Borel, A. Grandin, and B. Raveau, *Acta. Crystallogr. Sect. C* **46,** 2009 (1990).
15. D. Riou and M. Goreaud, *J. Solid State Chem.* **79,** 99 (1989).

16. G. Costentin, M. M. Borel, A. Grandin, A. Leclaire, and B. Raveau, *Acta. Crystallogr. Sect. C* **47,** 1136 (1991).
17. K. H. Lii and R. C. Haushalter, *J. Solid State Chem.* **69,** 320, (1987).
18. J. J. Chen, K. H. Lii, and S. L. Wang, *J. Solid State Chem.* **76,** 204, (1988).
19. G. Costentin, M. M. Borel, A. Grandin, A. Leclaire, and B. Raveau, *J. Solid State Chem.* **89,** 83 (1990).
20. C. Gueho, M. M. Borel, A. Grandin, A. Leclaire, and B. Raveau, *Z. Anorg. Alleg. Chem.* **615,** 104 (1992).
21. A. Guesdon, M. M. Borel, A. Grandin, A. Leclaire, and B. Raveau, *J. Solid State Chem.* **108,** 46, (1994).
22. A. Leclaire, T. Hoareau, M. M. Borel, A. Grandin, and B. Raveau, *J. Solid State Chem.,* **114,** 543 (1995).